6. ROCK NUCLEAR BEHAVIOUR & APPLICATIONS

6.1 GENERAL INTRODUCTION

6.2. NATURAL RADIOACTIVITY

- 6.2.1. Introduction
- 6.2.2. Radioactivity of Rocks
- 6.2.3. Gamma-ray detectors

6.3. THE GAMMA-GAMMA OR DENSITY APPLICATION

- 6.3.1. Introduction
- 6.3.2. Interaction of gamma-rays and atoms
  - 6.3.2.1. Compton scattering
  - 6.3.2.2. Photo-electric effect
  - 6.3.2.3. Pair Production
- 6.3.3. Density of the sedimentary rock
- 6.3.4. Photo-electric effect of the reservoir
- 6.3.5. Explanation of tools, environmental qualities and log readings
  - 6.3.5.1. Density tool configuration
  - 6.3.5.2. Mudcake compensation
  - 6.3.5.3. Density log characteristics
  - 6.3.5.4. Calibration
- 6.3.6. Applications of density logging tools

6.4. NEUTRON LOGS

6.1 GENERAL INTRODUCTION

Each element in the periodic table of elements has its own number of electrons, protons, neutrons and mass. As already discussed in chapter 3, the use of an electron charge on one spot gives a reflection product which consist of various wavelengths, with various amplitudes and (if needed) under various reflection angles. These factors can be used to identify specific elements or minerals (X.R.D., X.R.F., and Microprobe). In addition many elements are isotopes with specific decay times and related natural radiation or natural radioactivity. These properties can be measured with borehole- instruments, which can be divided into:

- a passive group groups that measures the **natural radioactivity,** usually by means of recording the gamma-rays that are emitted by elements in the formation, and,
- an active group, that contain both a radioactive source and detectors, and measures the **induced radioactivity** by means of a radioactive source. This source emits neutrons or gamma rays that penetrate the borehole and the surrounding formation.

In contradiction to electric logs, which are described in the previous chapter, the radioactivity or nuclear logs can be used through well casing.

Three types of radioactivity borehole-measurement apparatuses are normally used in combination:

1. **The gamma-ray application.**
   It is used to distinguish argillaceous rocks from non-argillaceous rocks. The first group shows to be more radioactive. Nevertheless, feldspathic sandstones, which are originally from igneous rock (high K-content in granite, gneiss, etc.), can be highly radioactive when compared to neighbouring shales. Consequently in clastic basins with much feldspathic sandstones the usefulness of the gamma-ray curve is reduced.
2. **The gamma-gamma, or density application.**
   It is used for rock porosity determination. A high-velocity gamma radiation source is pushed at a borehole wall and the rays are emitted into the formation. The amount of backscattering of the gamma radiation created by collisions with the mineral electrons, is measured. This measurement is directly related to the electron density and by that to the true bulk density. Further it is inversely related to the porosity.
3. **The neutron application.**
   Neutrons are able to follow the abundance of hydrogen nuclei in fluids, or, the higher the content, the lower the reading. All solutions in and around a borehole accommodate hydrogen, which "consumes" neutrons. For that reason porous rocks give low counts. Neutron logging shows variations in carbonate porosities. Accordingly they are logged by compensated neutron-density logs. Differences between water, oil, and mud filtrate cannot be distinguished by neutron detection, because of the corresponding percentage of hydrogen nuclei. Conversely dry gas shows

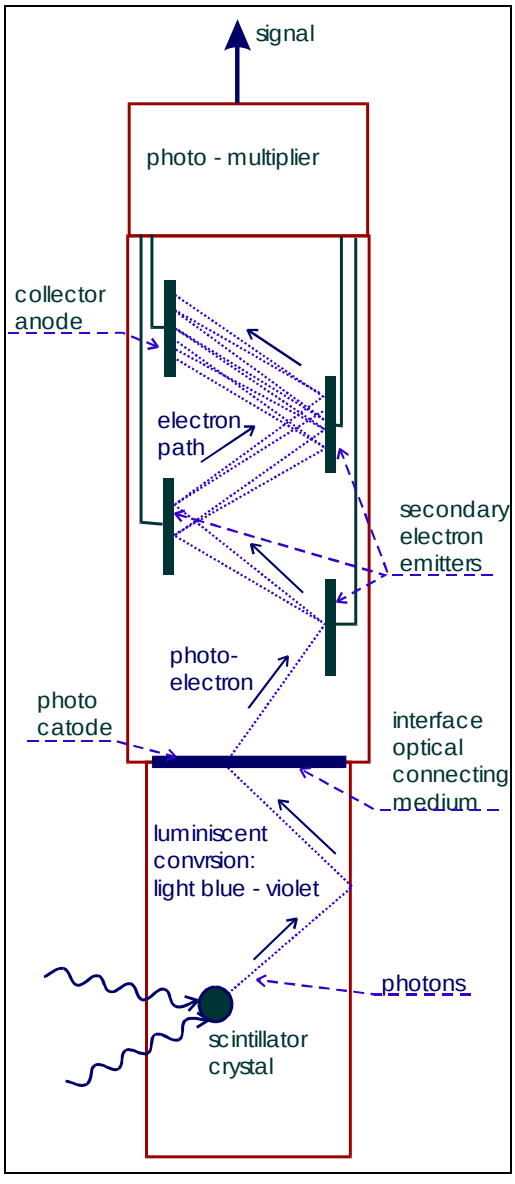

Figure 6. 1: Schematic view of a scintillator and photo-multiplier tube: The basic principle for gamma-ray detection

very high neutron readings; there are hardly any hydrogen nuclei in the gas phase when compared to the liquid phase.

In this chapter the principles of electron/neutron emission and registration are explained in relation to rock properties and tools for application. The methods are used in:

- Groundwater detection,
- Oil/gas exploration,
- Coal exploration
- Civil Engineering purposes (in other tool modifications; dredging, tunnelling, foundations, etc.)

6.2 NATURAL RADIOACTIVITY

6.2.1 INTRODUCTION

This section deals exclusively with natural radioactivity. Radioactivity is associated with the structure of the elements. An element contains protons and neutrons in its nucleus and electrons in one or more orbits. Its unique number of protons (Z) identifies each element. The majority of the elements consist of a mixture of two or more isotopes. Isotopes have the same number of protons but a different number of neutrons. Many isotopes are not stable and emit alpha, beta and/or gamma radiation, in order to permute to stable isotopes. Since beta- and alpha particles have a very limited penetration depth, often less than one cm in dense or heavy materials, the gamma-radiation is recorded with logging equipment in wells. Gamma rays, or photons, have a considerable penetration depth and even allow recording of natural gamma-radiation emitted by rocks through a steel casing.

6.2.2 RADIOACTIVITY OF ROCKS

Unstable elements of significant abundance that contribute to the natural gamma-radiation are:

- U-Ra : uranium-radium elements and their unstable daughter series of elements
- Th : thorium series
- K40 : potassium - 40 isotope.

The U-Ra and Th isotope series expose a wide range of energies, whereas Potassium - 40 radiates gamma rays with one single radiation energy (1.46 MeV). The radiation intensity (photons per gram per second) is shown in table 6.1

Radiation intensity photons/g.s	**Isotope series**
26000	U - RA
12000	Th
3	K^{40}

Table 6. 1: Radiation intensity of the main isotopes

The basic constituents of igneous rocks are:

- quartz, with a low degree of radioactivity
- feldspars and mica's, with K^{40} and sometimes U-Ra and Th

During rock weathering, sedimentological transport and diagenesis, feldspars decompose at a relatively rapid rate into clay minerals. Here radioactive-elements are trapped in the new minerals and the related rock structure. The Potassium content (0.02 vol.% of K^{40}-isotope) amounts to about 0.3% of ordinary clays (Table 6.2). As clay minerals are the

Lithology type	**Average Radioactivity in Radium Equivalent per Gram x 10^{-12}.**
Sand	4.1
Shaly and silty sand	7.1
Siltstone	10.3
Sandy shale	11.0
Shale	20.3
Black & grayish black shale	26.1
Calcareous sand	8.5
Limestone	3.8
Dolomite	3.1
Granite wash	6.9

Table 6. 2: Gamma-ray activities of sedimentary rock, from various sources.

principle constituents of shales, these are generally radioactive as well. Sometimes, in some shales, as much as 0.01 vol.% of U-Ra or Th is found. However, like most rules in geosciences, the previous mentioned general statements are hard and fast as well. Very good reservoir sands in some parts of the North Sea contain (Caledonian) mica, which contains a significant amount of radioactive potassium. They have a gamma-radiation level as high as the surrounding shales.

6.2.3 GAMMA-RAY DETECTORS

In the first measuring instruments Geiger-Müller tubes were used to detect gamma rays. These tubes have the disadvantages that the count-rates are low and that the output is not proportional to the energy of the individually detected gamma photons. Since the sixties scintillation counters are used to measure radioactivity in boreholes. These counters are based on the physical phenomenon that gamma rays, which interact with the crystal lattice, can produce secondary radiation, even in the visible light (florescence). The principle is depicted in figure 6.1. The most widely used material is Ta activated sodium iodide NaI. Other materials such a BGO (bismuth-germanium-oxide) and GSO (Gadolinium oxy-ortho-silicate) gain in popularity due to their higher density, and therefore more efficient conversion of gamma rays to scintillation.

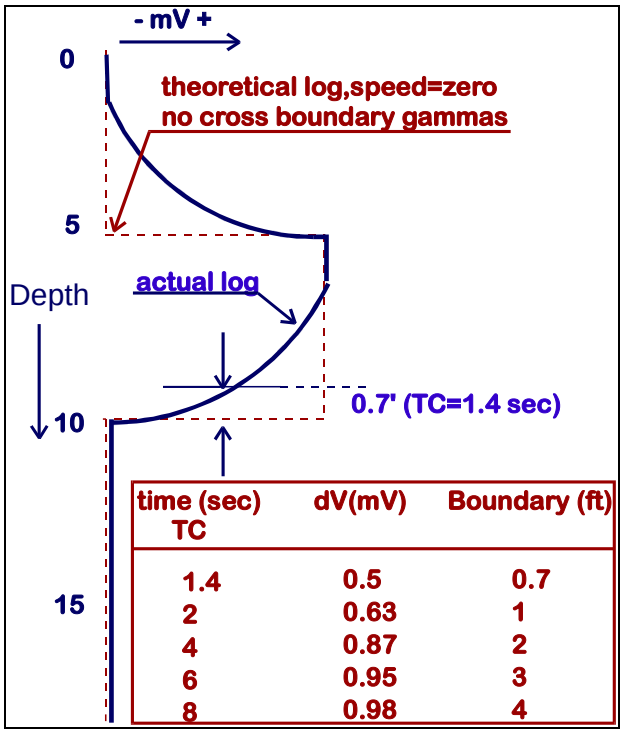

Figure 6. 2: Example of a boundary displacement gamma ray reading

The crystals are coated with a reflecting layer and the light quanta will therefore eventually hit the photo-cathode of a photo-multiplier where they dislodge one or more electrons. These electrons are in turn accelerated by a cascade circuit of electrodes, where each subsequent electrode has a higher voltage, and dislodge more electrons at each stage. This multiplication process leads to an avalanche of electrons that produce a measurable electric pulse at the last anode of the tube. An attractive feature of this technique is that the pulse height is proportional to the energy of the original gamma-photon.

Logging speed (ft/hr)	3600	1800	1800	900
Time constant, (sec)	5	5	2	4
Statistical variations	low	low	fair	low
Travel during TC, ft	5	2.5	1	1
Thin bed definition	poor	poor	good	good

Table 6. 3: Logging speed versus log quality for the GR

Radioactive emissions are random phenomena, which vary in time and create statistical fluctuations of a gamma-ray log. In order to minimise the fluctuations, averaging is applied. In the past this was accomplished by an simple resistivity-capacitor (R-C) circuit, nowadays the averaging is carried out digitally from an analogue to a digital (A-D) conversion. A time-averaging constant TC is applied to smooth the gamma-log. The faster the tool moves through the hole the less gamma's will be counted per depth unit, and the longer time averaging period has to be to smooth out the statistical fluctuations. A theoretical example (figure 6.2) shows, for a logging speed of 1800 ft/hr and a time-averaging constant TC = 2 sec, that the time lag produces an apparent boundary displacement of about 1 foot. The averaging procedure causes a time lag on the log boundaries which increases with logging speed and TC as demonstrated in the table placed in figure 6.2. The selection of the TC is a practical

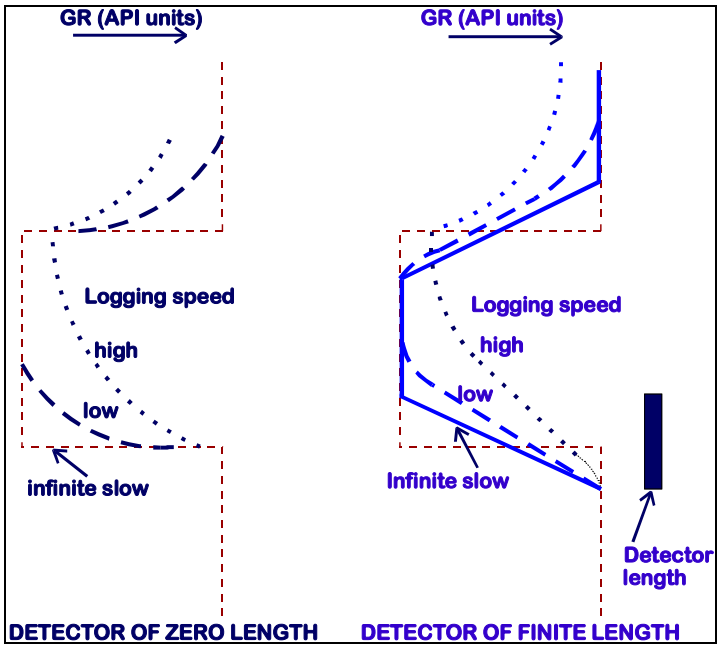

Figure 6. 3: Effects of detector length and logging speed on the shape of the gamma ray log.

compromise of logging speed and log quality (see table 6.3). The normally used standards are a speed of 1800 ft/hr and a TC of 2 sec. The parameters listed in the last column of table 6.3. can be used over short intervals for a good bed or an explicit layer definition. It is customary to maintain the product of logging speed (ft/sec) and TC (sec) at one foot. Figure 6.3 shows the GR log shapes as a function of logging speed for a fixed TC of 2 sec.

The investigation volume of the Gamma Ray tool has the shape of a sphere around the detector. The depth of investigation is determined by:

- The rock density and mud density which attenuate the gamma-rays
- The natural gamma ray energy
- The detector length; 4", 8", and occasionally 12"

An approximate value for the vertical resolution is 2 feet. The depth of investigation is about 1 foot. In figure 7.3 the effect of the detector size on the vertical resolution is explicated.

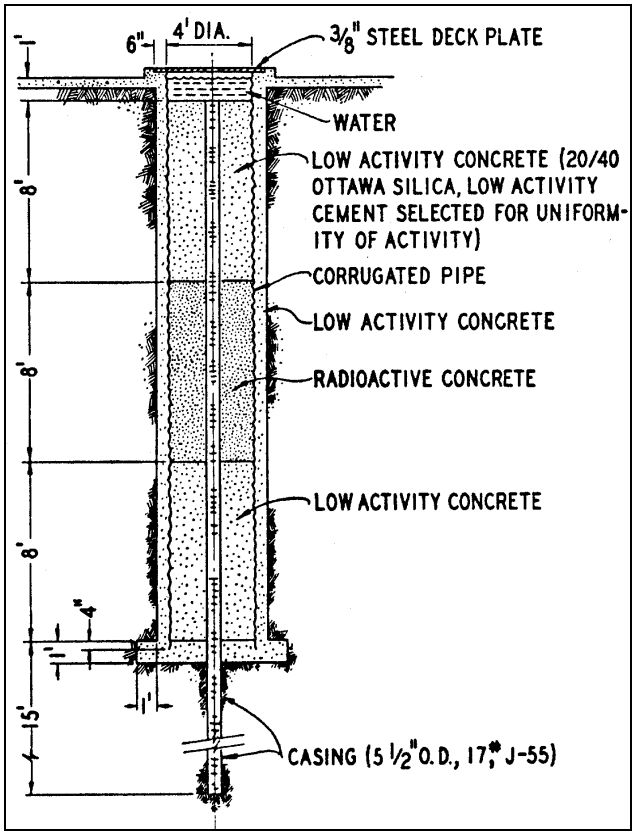

Figure 6. 4: Schematic view of the gamma ray log calibration pit.

6.2.4 CALIBRATION

The unit of gamma-ray intensity is defined by a standard calibration procedure carried out in the test pit of the University of Houston Texas (figure 7.4). The API Gamma Ray unit is 1/200 of the difference in log deflection between the two zones of different Gamma Ray intensity. In the test pit a combination of radioactive concrete with 13 ppm U, 24 ppm Th, 4% K (mica), and a layer with very low radioactive concrete is used to define this unusual API "unit". For calibration at the well site, to check the API reading, one uses a small radioactive source placed at a fixed distance from the detector.

6.2.5 THE CALCULATION OF SHALE VOLUMES

The more or less linear behaviour of the natural gamma ray increase with the increase of clay or shale, by the presence of potassium, gives the opportunity to calculate the shale/clay-content in K-feldspar free sands. With the natural gamma ray log readings the shale volume V_{sh} can be calculated as follows:

$$V_{sh} = \frac{GR - GR_{min}}{GR_{sh} - GR_{min}} \qquad \text{(eq. 6.1)}$$

With; GR as the actual log reading corrected for environmental influences; Gr_{min} as the gamma ray reading in a clean (with no shale) interval, and; GR_{sh} as the gamma ray reading in a 100 % shale interval

An example is given in figure 6.5. This linear relation between V_{sh} and GR reading usually gives a pessimistic (too high) shale volume.

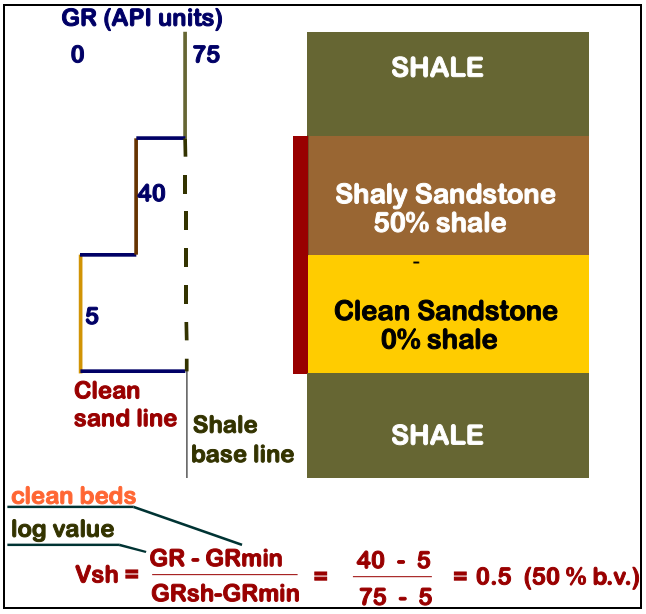

Figure 6. 5: Example of a shale volume calculation, using a clean sand and the shale base line.

6.2.6 INTERPRETATION OF ENVIRONMENT

As shown with the SP-readings, a consistency in mineral content gives the opportunity to translate a series of log readings to a rock type or even a sedimentary environment. Moreover, with various log readings it is also possible to make correlations between wells, or in one well through time. Figure 6.6 shows the log readings of various examples of sediment types and related sedimentary environments. furthermore it shows parallel the differences between gamma ray readings and neutron readings.

6.2.7 APPLICATIONS OF THE NATURAL GAMMA-RAY LOG (GR)

The main applications of the GR in lithology determination are:

- obtaining information on clay typing and shale volume estimates
- delineating reservoir rock (sand / shale separation)
- determination of the ash content of coal seams
- well-to-well correlation of GR logs to recognise layer (dis-)continuities
- depth correlation of different logging runs carried out:
  - ➔ in one well,
  - ➔ through a casing,
  - ➔ as a correlation between production logs,
  - ➔ for perforating guns,
  - ➔ for formation testers, and,
  - ➔ for open hole logs.
- the indication of environment of deposition and its lateral extension (comparable with SP log applications).
- detection of radioactive evaporites - sylvite (KCl)

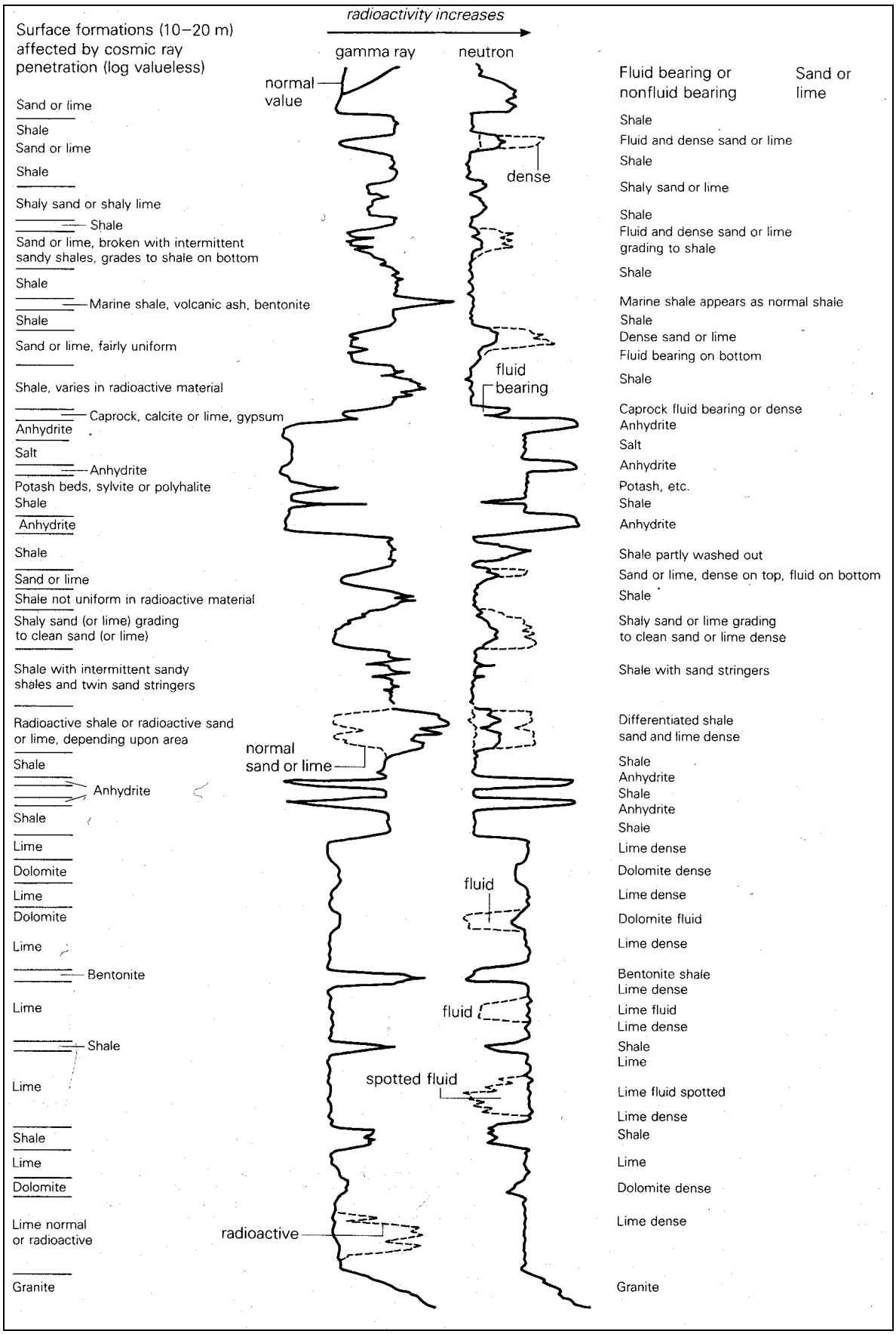

Figure 6.6: Gamma-ray and gamma-gamma log readings. Examples from various sedimentary environments

6.3 THE GAMMA-GAMMA, OR DENSITY APPLICATION.

6.3.1 INTRODUCTION

In contrast to the gamma ray, which only contains a passive detector, the density tool contains a chemical gamma-ray source, consisting of the isotopes Caesium 137 or Cobalt 60, and two ore more gamma-ray detectors. The density tool is therefore called an induced gamma or gamma-gamma tool. The induced gamma rays are scattered by the rock and only a few reach one of the gamma-ray detectors in the tool (figure 6.7). The basic principle shows that a higher density of the rock material will attenuate more of the gamma rays and less will reach the detectors. The use of the gamma-gamma tool for density measurements is based on this attenuation phenomenon.

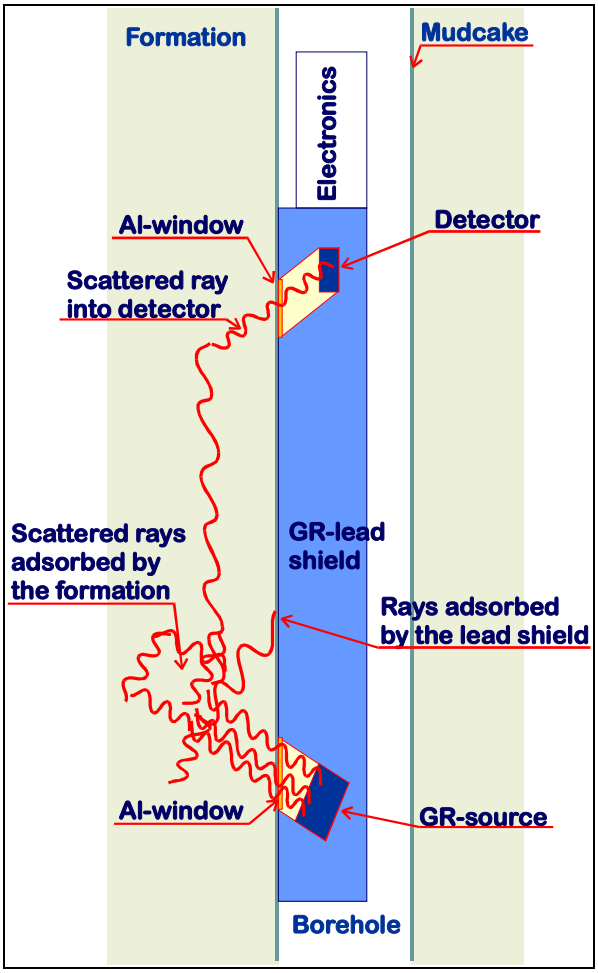

Figure 6.7: A sketch of a single gamma-gamma density tool

6.3.2 INTERACTION OF GAMMA-RAYS AND ATOMS

There are 3 ways for an atom to interact with gamma rays as depicted in figure 6.8:
1: Compton scattering
2: Photoelectric effect
3: Pair production

6.3.2.1 COMPTON SCATTERING

The high-energy gamma rays emitted by the source collide with the electrons in the formation. At each collision the photon loses some of its energy to an electron, which can be ejected from its orbit. The scattered gamma ray has less energy than the gamma ray that caused the collision, and the energy level of the scattered gamma ray is strongly dependent on the collision angle. When the number of gamma rays is recorded as a function of their energy in a frequency vs. energy diagram an energy spectrum is obtained. The energy spectrum of the scattered gammas is the well-known Compton continuum.

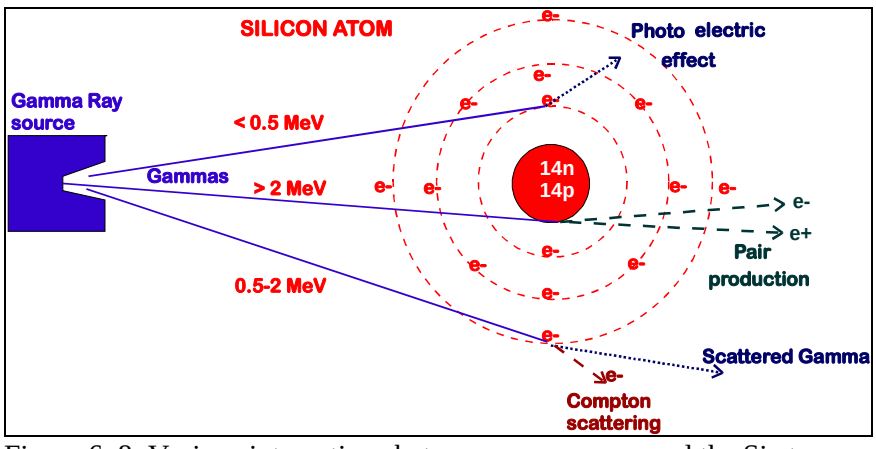

Figure 6. 8: Various interactions between gamma rays and the Si atom

6.3.2.2 PHOTO-ELECTRIC EFFECT

After several collisions the gamma rays that result have lower energies (< 0.5 MeV). Below this energy level, the photoelectric effect becomes predominant. Then the gamma rays can interact with the electrons of the inner bands. The gamma energy is used to push an electron into a higher

band. If the electron falls back to the original band gamma rays are emitted with energies characteristic for the atomic number.

6.3.2.3 PAIR PRODUCTION

In this process the high energy photon (>2 MeV) looses all it's energy and the gamma-ray is converted into an electron and a positron. The positron combines almost immediately with another electron and two gamma rays each with an energy of 1.04 MeV are emitted in opposite directions. The density tools use sources that emit gamma rays with energies below 2 MeV, hence pair production will not be further discussed in the context of gamma-gamma logging.

When a beam of gamma-rays with initial intensity I_0 is scattered by a slab of material with thickness "x" resulting in an intensity I at the other side of the slab, the following relation is valid :

$$I = I_0.e^{-\mu.x} \qquad \text{(eq. 6.2)}$$

or

$$ln\frac{I}{I_0} = -\mu.x \qquad \text{(eq. 6.3)}$$

In other words, the logarithm of the ratio of intensities of the attenuated and the original beams is proportional to a) the slab thickness and b) a proportionality factor μ. Here μ is defined as the mass absorption coefficient. In figure 6.9 the mass absorption coefficient, expressed in cm^2/g, is plotted against the energy of the gamma rays. The lines indicate the probability that one of the three interactions described above will occur as a function of the gamma-ray energy.

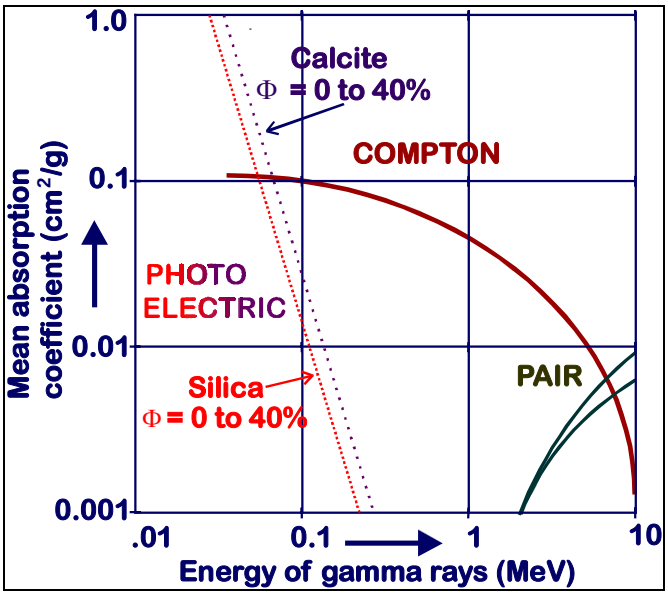

Figure 6. 9: Gamma ray mass absorption coefficient over the energy range of interest. (Revised after Tittman and Wahl, 1965)

6.3.3 DENSITY OF THE SEDIMENTARY ROCK

At the distance of some 20 - 30 cm between source and detector the gamma rays usually scatter two to three times before some of them reach the detector. The number of collisions between the electrons and gamma's is directly related to the number of electrons in the formation. A low count is indicative for a high number of electrons and thus for a high-density formation. In essence, the response of the density tool is determined by the electron density ρ_e that is related to the bulk density as follows:

$$\rho_e = \frac{N.Z.\rho_b}{A} \qquad \text{(eq. 6.4)}$$

with:

ρ_e : electron density in number per volume unit
N : Avogadro's number as $6.03 * 10^{23}$ atoms per gram atom
Z : atomic number or number of protons, which is dimensionless
ρ_b : as the bulk density, in $g.cm^{-3}$
A : as the atomic weight, which is related to number of protons and neutrons

The bulk density depends on the density of the rock material, porosity and the densities of the different phases of oil, gas and water that are present in the pore space. For most formation substances the factor 2 (Z/A) is very close to unity (for hydrogen close to 2), as demonstrated in Table 6.4. The resulting apparent bulk density ρ_a, as seen by the tool, is related to the electron density ρ_e:

$$\rho_a = 1.07.\rho_e - 0.188 \qquad \text{(Eq. 6.5)}$$

For liquid filled sandstone, limestone and dolomite the tool that is reading ρ_a is practically identical to the actual density ρ_b, as shown in table 6.5. Corrections are required e.g. in anhydrite, sylvite, halite and also in gas bearing formations. For a number of minerals the chemical and other physical characteristics are also given.

Element	A	Z	2 Z/A
H	1.008	1	1.9841
C	12.011	6	.9991
O	16.000	8	1.0000
Na	22.99	11	.9569
Mg	24.32	12	.9868
Al	26.98	13	.9637
Si	28.09	14	.9968
S	32.07	16	.9978
Cl	35.46	17	.9588
K	39.10	19	.9719
Ca	40.08	20	.9980

Table 6. 4: 2Z /A values for various elements

Compound	Formula	Actual	2SUM(Z's)	Electron	Apparent
		density ρ_b	molar weight	density ρ_e	density (tool) ρ_a
Quartz	SiO_2	2.654	0.9985	2.650	2.648
Calcite	$CaCO_3$	2.710	0.9991	2.708	2.710
Dolomite	$CaCO_3$, $MgCO_3$	2.870	0.9977	2.863	2.876
Anhydrite	$CaSO_4$	2.960	0.9990	2.957	2.977
Anth. coal		1.4-1.8	1.030	1.442-1.852	1.355-1.796
Bitum. coal		1.2-1.5	1.060	1.272-1.590	1.173-1.514
Fresh water	H_2O	1.000	1.1101	1.110	1.00
Salt water	200.000 ppm	1.146	1.0797	1.237	1.135
"Oil"	n(CH_4)	0.850	1.1407	0.970	0.850
Methane	CH_4	ρ_{met}	1.247	1.247 ρ_{met}	1.335 ρ_{met}-0.188
"Gas"	$C_{1.1}$ $H_{4.2}$	ρ_g	1.238	1.238 ρ_g	1.325 ρ_g -0.188
In which ρ_{meth}, and ρ_g are the density of methane and composite gas respectively.					

Table 6. 5: Values related to the density tool (After Serra, 1984)

6.3.4 PHOTO-ELECTRIC EFFECT OF THE RESERVOIR

The photoelectric effect P_e curve is an index of the effective photoelectric absorption cross section of the formation. The unit of the photoelectric absorption cross section τ is in barns (10^{-24} cm^2) per atom. As mentioned in the introduction the gamma rays of the photoelectric effect are produced when electrons in the inner bands return to their original state. The energy of these gamma rays is therefore dependent on the binding forces of electrons in the inner bands and strongly dependent on the atomic number *Z*:

$$\tau = K.Z^{4.6} \qquad \text{(Eq. 6.6)}$$

τ : Photoelectric absorption cross section in barns per atom
Z : atomic number
K : a "relative" constant

The coefficient K varies with the energy level of the incident gamma rays. Dividing τ by Z and calibrating the P_e log such that K is arbitrarily taken as $E^{-3.6}$, gives:

$$P_e = (Z/10)^{3.6} \qquad \text{(Eq. 6.7)}$$

Where, P_e is again the effective photoelectric absorption cross section, but now expressed in barns/electron.

To obtain a parameter that is proportional with the volume fractions of the formation constituents P_e is multiplied with the electron density. This yields the effective photoelectric absorption cross section index per unit volume $U=P_e.\rho_e$. Then the relative volumes of the rock and pore components can describe the formation:

$$U = \varphi.U_{fl} + (1-\varphi).U_{ma} \qquad \text{(eq. 6.8)}$$

The effective photoelectric absorption cross section per unit volume "U" is, as demonstrated by the equations 6.7 and 6.8, strongly dependent on the atomic number and therefore an excellent lithology indicator.

6.3.5 EXPLANATION OF TOOLS, ENVIRONMENTAL QUALITIES AND LOG READINGS

6.3.5.1 DENSITY TOOL CONFIGURATION

In order to minimise the influence of the mud column the tool features two or more gamma-ray detectors. A configuration with two detectors at approximately 8 and 16 inches from the source is shown in figure 6.10. Both the detectors and the source are mounted on a skid and shielded from the borehole. The skid, which has a plough-shaped leading edge to remove part of the mudcake, is pressed firmly against the wall by means of an eccentring arm. The two detectors are necessary to account for remaining mudcake or mud interposed between the skid and the formation. The litho-density tool (LDT) offers a combination of the density and the photoelectric absorption P_e measurements.

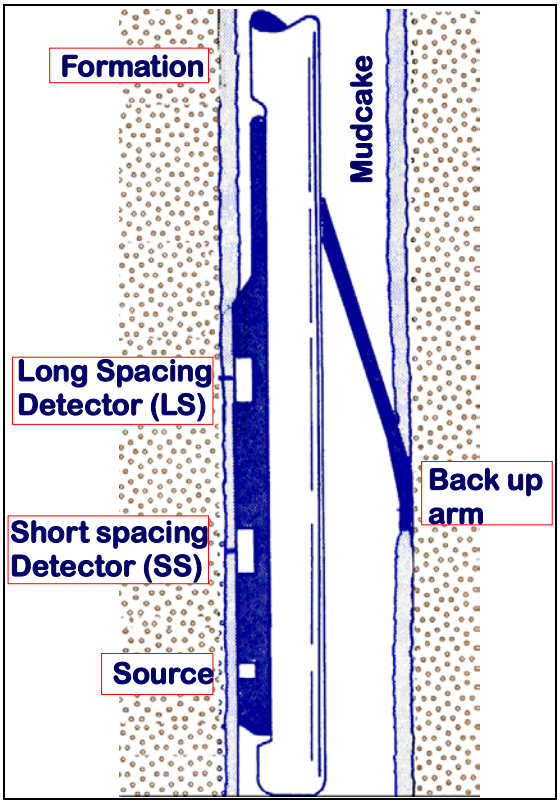

Figure 6. 10: Dual-spacing formation density log (revised after Schlumberger)

6.3.5.2 MUDCAKE COMPENSATION

Although the source and detectors are pressed against the borehole wall, there are small washouts and irregularities called hole rugosity that will affect the gamma-ray attenuation. Moreover, normally there is a thin layer of mudcake between the skid and the borehole wall. Since the two detectors have a different depths of investigation due to their short (SS) and long (LS) spacing from the source, the wash-outs and mudcake have a different effect on the SS and LS detector responses. By combination of the two responses the effect of the mudcake and small washouts can be compensated. This method is called the "spine- and ribs correction", and has been automated and incorporated in the surface computer. The density readings displayed on the log shown in figure 6.11, have already been

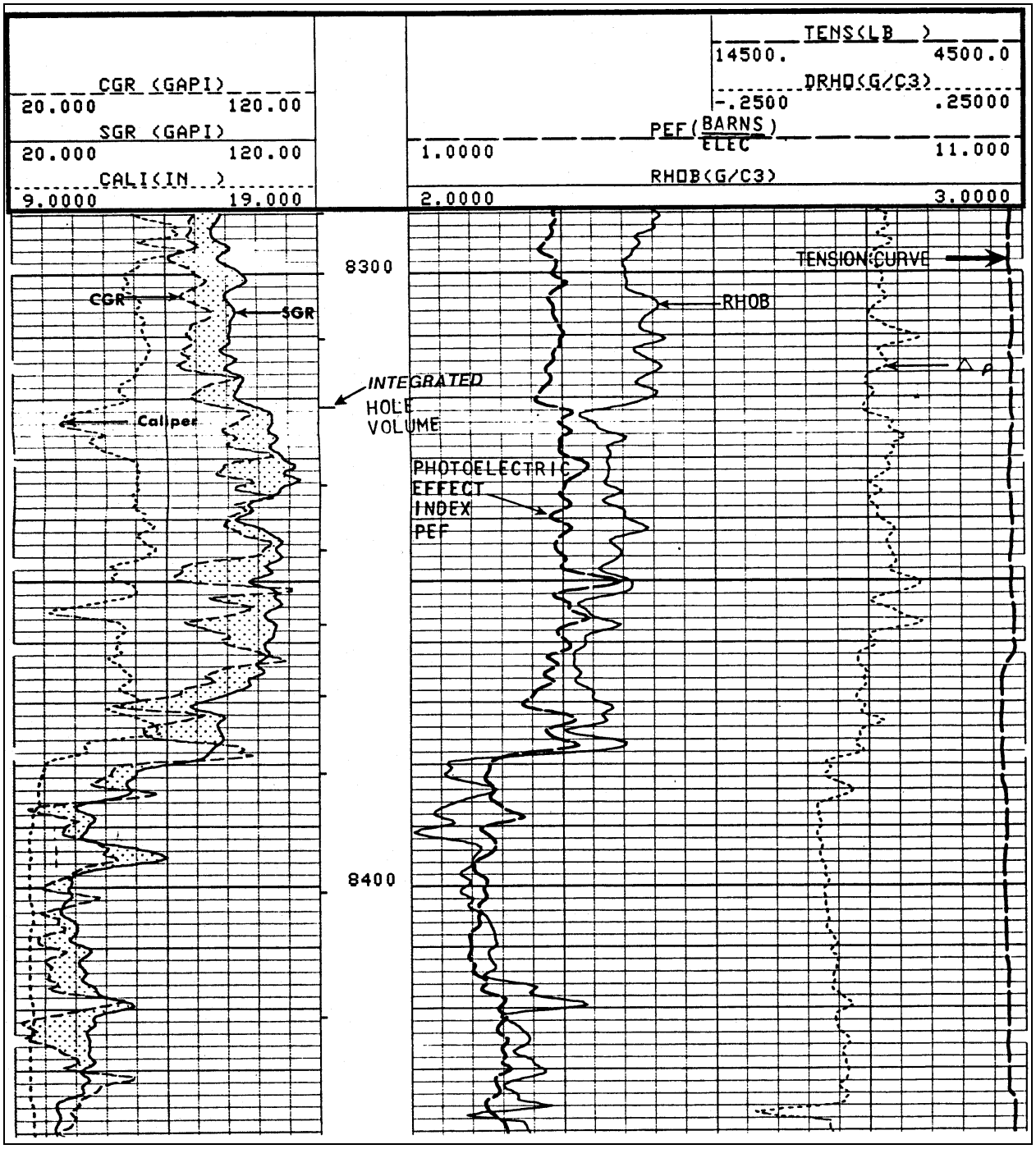

Figure 6. 11: An example of a litho-density log as can be expected from Schlumberger.

compensated with the correction $\Delta\rho_b$. This is the difference between the densities provided by the LS and SS detectors.

6.3.5.3 DENSITY LOG CHARACTERISTICS

The actual density measurement and the P_e photoelectric effect curve are usually recorded in tracks 2 and 3 of the log as shown in figure 6.6. The first track is customarily reserved for the natural gamma curve together with the calliper of the density tool (extension of back-up arm shown in figure 6.10). The horizontal depth of investigation is quite shallow; approximately 6 inches. Accordingly, in many permeable formations the log only measures in the flushed zone. The vertical resolution of the tool is about 1 ft.

6.3.5.4 CALIBRATION

The **primary calibration standards** for the density tools are laboratory fresh-water-filled limestone formations of the test pit at the Houston University discussed in the previous section (figure 6.4). The **secondary standards** are large aluminium and sulphur blocks into which the sonde is inserted in the field workshop of the logging contractor. With the blocks two different thicknesses of artificial mudcake are used to check the automatic mudcake correction. At the well site a radioactive test jig produces a signal of known intensity in order to check the detector response. Normally the best checks are:

- comparison of repeat section with the original log curve
- calibration in typical pure deposits like anhydrite with a density of 2.98 g/cc.

6.3.6 APPLICATIONS OF DENSITY LOGS

The Formation Density log has several practical applications:

- porosity calculation
- acoustic impedance determination; the density combined with the sonic travel times gives the acoustic impedance. This is important for calibration of seismic signals
- identification of various evaporites
- gas detection in reservoirs

The P_e curve is a good lithology indicator. The influence on the P_e of the reservoir porosity and fluid content, including gas, is insignificant.

6.4 NEUTRON LOGS

6.4.1 INTRODUCTION

Neutron tools were the first logging instruments that used radioactive sources to determine the porosity of the formation. After the later introduction of the gamma-gamma density tool, the neutron log was used to correct the density porosity readings for the effects of shale and gas. The neutron tool response is dominated by the amount of hydrogen atoms present in the formation (figure 6.12). If the rock material contains little hydrogen (thus no high shale contents) and the fluid in the pore space is either oil or water (thus the hydrogen index = 1), then the neutron log response is a good measure for the porosity. For the assessment of porosity in gas bearing formations and shaly members or formations, a combination of the neutron tool and density tool is often required. The big advantage of neutrons, i.e. to travel through steel casing and cement, gives the opportunity to acquire porosity information and hydrocarbon saturations in cased holes[1].

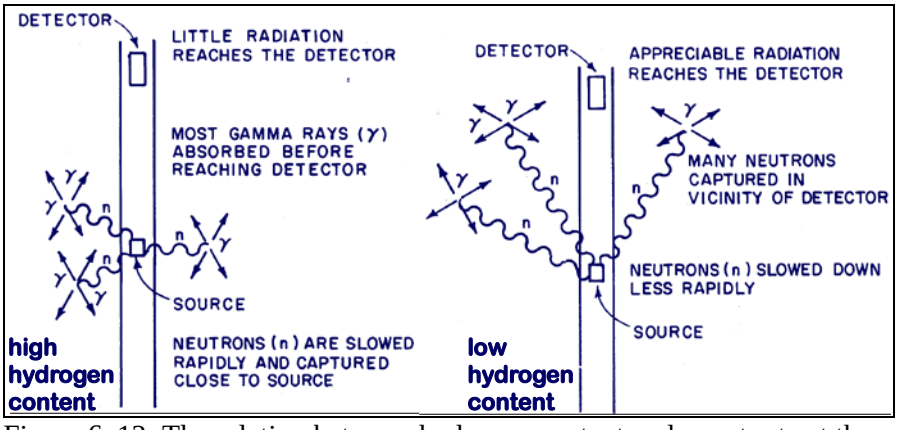

Figure 6. 12: The relation between hydrogen content and count rate at the detector. Left; a high content, right; a low content

[1] This section is restricted to open hole applications.

6.4.2 THEORETICAL BACKGROUND

6.4.2.1 BASIC CONCEPT

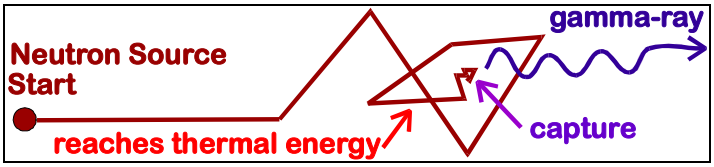

Figure 6. 13: Emission, travelling and collisions of a neutron in a formation

The electrically neutral neutrons have a mass, which is practically identical to that of hydrogen atoms. The neutrons that are emitted from a neutron source have a high energy of several MeV. After the emission they collide with the nuclei of the borehole fluid and formation materials. With each collision the neutrons loose some of their energy (figures 6.13 & 6.14). The largest loss of energy occurs when the neutron collides with a hydrogen atom. Therefore the slowing down of the neutrons largely depends on the amount of hydrogen in the formation. The first free path length is the longest successive path length-decrease until the neutrons reach thermal velocities with a thermal energy of about 0.025 eV. At this energy level the neutrons are in thermal equilibrium with the other nuclei in the rock formation. Sooner or later the neutrons are captured with the emission of a capture gamma ray. The amount of energy lost at each collision depends on the relative mass of the target nucleus, and the scattering cross section. In other words, it depends on the probability for collision of a neutron with a nucleus (fig. 6.14). The principles of the neutron tools are summarised as follows :

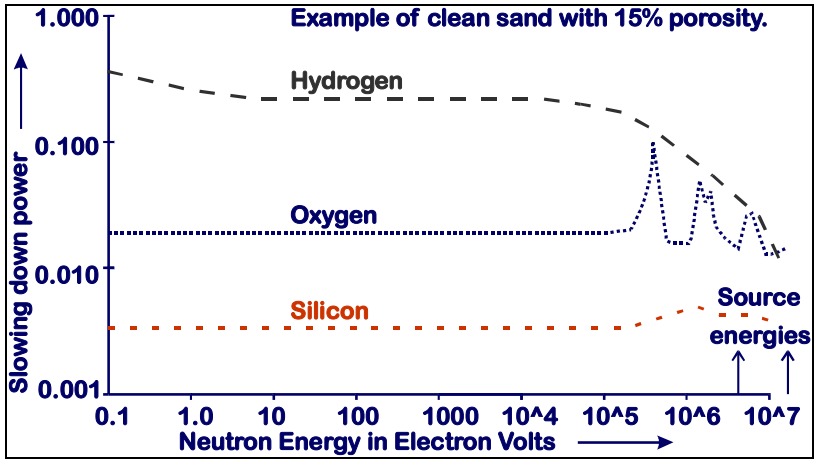

Figure 6. 14: Slowing down power of H, O, Si for different neutron energies

- a neutron source emits a continuous flux of high energy neutrons
- collisions with formation nuclei reduce the neutron energy
- at thermal energy level (ca 0.025 eV.) neutrons are captured
- neutron capture results in an emission of gamma rays
- the detector measures the slowed down neutrons and/or emitted gamma rays

Energy loss is greatest when neutrons collide with hydrogen atoms. Figure 6.15 illustrates the slowing-down process. Depending on the type of tool, either the so-called capture gamma rays, the epi-themal or the thermal neutrons that reach a detector are counted.

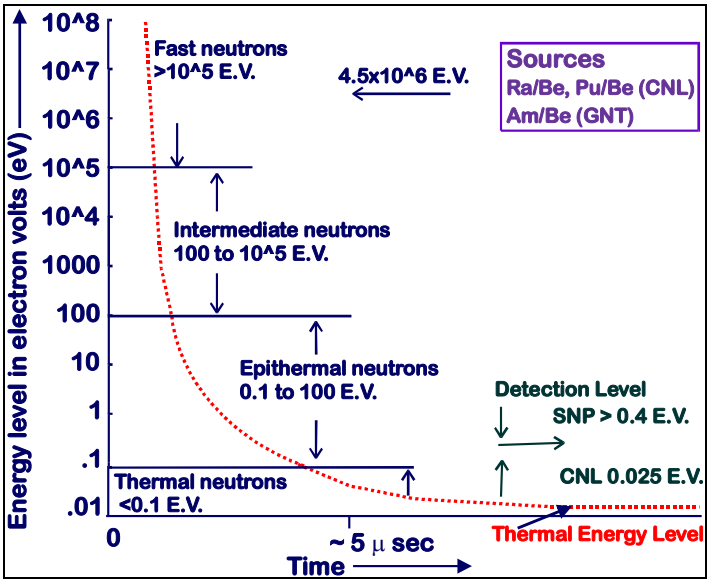

Figure 6. 15: Neutrons energy level versus time, showing decay after leaving the source.

6.4.2.2 HYDROGEN INDEX

The H-concentration has been defined in terms of a Hydrogen Index (HI), which is proportional to the quantity of H atoms per unit volume. The hydrogen index of fresh water at surface conditions is taken as the unity.

$$HI = \frac{number\ of\ H\ atoms}{(volume\ ).(number\ of\ H\ atoms\ in\ 1\ cc\ H_2O)} \qquad \text{(eq. 6.9)}$$

- For a paraffinic oil (nCH_2) we find $HI_{(oil)} = 1.29.\rho_{(oil)}$. If the in situ density of this oil is 0.78 g/cc, its hydrogen index is equal to that of water which has, as mentioned by definition, a value 1.
- For methane (CH_4) the hydrogen index depends strongly on the gas pressure. A typical value for HI_{CH4} at 100 bar is 0.225.

Since the zone of investigation of the neutron tool is often confined to the flushed zone, the porosity derived from the Neutron log (ϕ_n) is related to the true porosity (ϕ) by the equation (figure 6.16):

$$\varphi_n = \varphi.(HI_{mf}.S_{xo} + HI_{hc}.(1 - S_{xo})) \qquad \text{(eq. 6.10)}$$

In the above quoted case of the paraffinic oil with a density of 0.78 g/cc density we find $\phi_n = \phi$
In the case of CH_4 with in-situ density 0.1 g/cc and flushed zone water saturation S_{xo} of 0.7 we find :

$$\varphi_n = \varphi.(1*0.7 + 0.225\ *\ 0.3) = 0.77*\varphi \qquad \text{(eq. 6.11)}$$

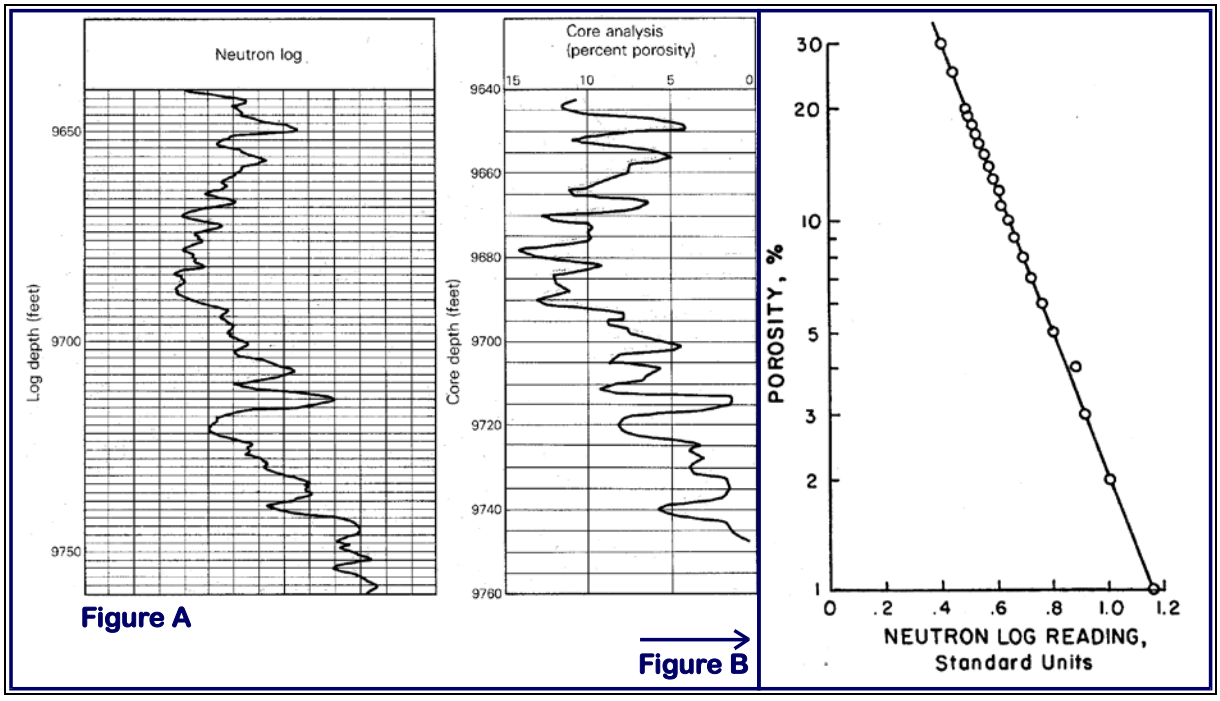

Figure 6. 16: Porosity/neutron log reading correlation. A: Neutron logs readings correlated with laboratory porosities, B: Neutron logs readings versus porosities.

6.4.3 TECHNICAL ASPECTS AND VARIETY IN NEUTRON TOOLS

6.4.3.1 PRINCIPALS AND TECHNICAL HISTORY

The neutron tools that pick up capture gamma rays are equipped with NaI-detectors. These detectors are also used in the natural gamma-ray tool and the density tool. If the neutron tool detects neutrons HeF-tubes, based on the same principles as Geiger Müller tubes, are applied. Epi-thermal neutrons are preferentially detected by shielding the HeF-detectors from thermal neutrons with a thin boron layer on the outside of the detector. The evolution of neutron tools is as follows :

GNT : 1950's - responds to capture gamma rays and thermal neutrons (Am-Be source).
SNP : 1960's - responds mainly to epi-neutrons with energy level > 0.4 eV, detector shielded.
CNL-C: 1970's - responds to thermal neutrons, capture gammas are recorded.
CNL-G: 1980's- contained two sets of two thermal and epi-thermal neutron detectors.
APS : 1990's- has an array of one thermal and two pairs of epi-thermal neutron detectors.

6.4.3.2 CHEMICAL SOURCES

The chemical neutron sources usually consist of a mixture of beryllium (Be) and an alpha emitting radioactive element Radium (Ra), Plutonium (Pu), or Americium (Am). In the mentioned tools the following natural radioactivity reactions take place:

1. Radium decays to Radon and Helium:

$$ {}_{88}Ra^{226} \longrightarrow {}_{86}Rn^{222} + {}_{2}He^{4} \qquad \text{(eq. 6.12)} $$

2. The alpha particles from Helium (He) bombards the Beryllium target and both neutrons and gamma rays are produced:

$$ {}_{4}Be^{9} + {}_{2}He^{4} \longrightarrow {}_{6}C^{12} + {}_{o}n^{1} + \text{gamma rays.} \qquad \text{(eq. 6.13)} $$

3. Within a few microseconds the neutrons are slowed down to the thermal energy level, as shown in the figure 6.13 and 6.15. After that they normally are captured by H- or Cl-nuclei in a process that can take up 1000 μs. The capturing nucleus becomes exited and emits gamma rays, e.g.:

$$ {}_{1}H^{1} + {}_{o}n^{1} \longrightarrow {}_{1}H^{2} + \text{gamma rays} \qquad \text{(eq. 6.14)} $$

The detectors are located at distances less than 1 feet and 2 feet from the source. The detector distances in the neutron tools[2] are chosen in such a way that the neutron density around the detector is low when the hydrogen content of the formation is high. In other words the hydrogen atoms in the formation act as a shield to keep the neutrons away from the detectors. **Thus,** the count rate of neutrons or gamma rays produced by thermal neutron capture is therefore *LOW* in *HIGH* porosity rocks that contain oil or water. When dealing with a low porous rock the neutrons can penetrate deeper into the formation and the count-rate around the detector will be higher. If gas, which has a very low hydrogen content, is present, then the neutrons will penetrate deeper and the count rate will be higher compared to a water or oil filled rock with the same porosity and matrix composition. Gas will give the erroneous impression that a low porosity formation is logged.

Another source type is the *accelerator (minitron) neutron source*. This non-chemical source will be discussed in the section of the accelerator porosity sonde (section 6.4.3.5).

[2] with the exception of the accelerator porosity sonde **(**APS)

6.4.3.3 SIDE-WALL NEUTRON POROSITY TOOL (SNP)

The SNP tool is designed for operation in the open hole. The source and the "one" detector are placed in a skid, 16 inches away from each other, using a configuration that resembles the density tool.

- The detector is shielded from thermal neutrons with a boron compound.
- The skid is applied to the borehole wall to minimise borehole and mudcake effects.
- The advantages of the SNP tool are that the log can be recorded simultaneously with the density log, and that the log is much less sensitive for shale because it detects epi-thermal neutrons instead of capture gamma rays.
- The disadvantage is the use of only one detector that prevents correction of remaining mudcake and borehole effects.

The tool was very successful in combination with the density tool in detecting gas. It was withdrawn due to its low logging speeds that were necessary due to the low epi-thermal neutron count rate.

6.4.3.4 COMPENSATED NEUTRON LOG (CNL)

The CNL tool from Schlumberger, and equivalent models from other logging contractors, is the most widely used neutron-logging tool at the early 90's. As shown in figure 6.17, the **CNL-C** version is equipped with 2 detectors, which are sensitive to thermal neutrons.

- The detectors are located at 15 and 25 inches from the source. The far detector has a larger volume than the near one in order to maintain adequate count rates.
- The tool measures the rate at which the thermal neutron population decreases from the near to the far detector.
- A very strong neutron source (16 Curie) reduces statistical variations and permits longer spacings. This in turn increases the zone of investigation.
- Furthermore, the effect of borehole is reduced as shown in the figure. The tool can be run in cased and open liquid filled holes.
- A large bow-spring ensures eccentring of the tool and optimum contact with the borehole wall.

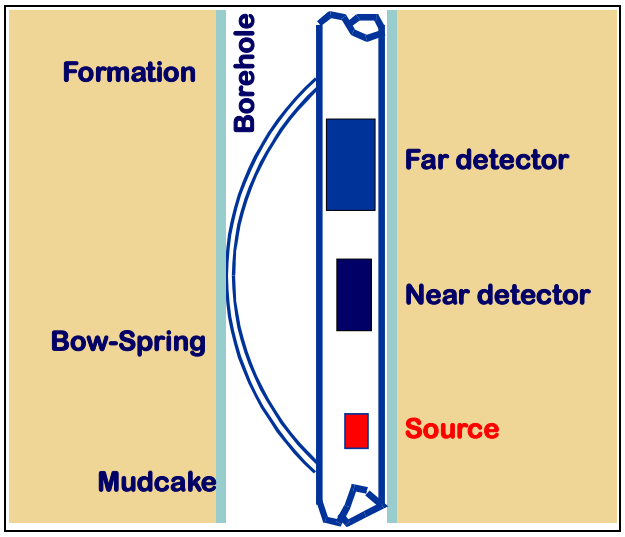

Figure 6. 17: Lay-out of the CNL tool

The **CNL-G** version has two epi-thermal detectors in addition to the thermal detectors at the other side and closer to the source. Due too the low epi-thermal count rates, which led to low logging speeds, this tool is (except for special low speed operations) also out of use,.

6.4.3.5 ACCELERATOR POROSITY SONDE (APS)

In contrast with all foregoing neutron tools this instrument has an *accelerator (minitron) neutron source*, instead of a chemical source. The accelerator porosity sonde (APS) was partly developed to comply with stricter environmental and safety regulations, which are expected to be enforced in the near future. However the use of a pulsed neutron source, which has a very high output, also enabled the design of a tool that contains detectors at three different spacings. This construction produced a stable epi-thermal neutron, which can be run at logging speeds compatible with the density tool. The tool combines the responses of the various detectors to compensate for lithology and matrix density effects.

6.4.4 CALIBRATION

The primary standard for calibration is again a shallow hole at the University of Houston, called the API "neutron pit" (figure 6.4). For the out-of-date gamma-neutron GNT tool the response of the neutron tools in the 19 % porosity and water filled limestone was arbitrarily defined as 1000 API units. The primary standard of calibration for SNP, CNL, and APS tools is performed in limestone, sandstone and dolomite formations of high purity and accurately known porosity. The departure of the sandstone and dolomite calibrations from the reference limestone calibration is presented on charts provided by the contractor.

The wellsite calibration is carried out by means of an U-shaped polyethylene block with a two-position block, providing two different count rates, equivalent to 11 vol.% and 22 vol.% limestone porosity. The CNL is calibrated in the workshop in a calibrating tank. A calibrated test source is used at the wellsite. The repeat section recorded at the bottom of the hole is the best check for a reliable and repeatable log. Further checks can be made in a formation with a known lithology such as anhydrite and halite intervals (the theoretical CNL reading of 0 vol.% pore volume).

6.4.5 APPLICATIONS FOR NEUTRON TOOLS

The open hole neutron porosity logs have a multitude of applications:

- porosity determination usually in combination with the density tool
- gas detection usually combination with the density tool, but also with a sonic tool
- shale volume determination in combination with the density tool
- lithology indication again in combination with the density log
- Revised neutron tools are nowadays also in use to identify the type and extension of river/lake sediments for the controlled optimisation of dredging speed and control of mud/sand dumping sites.